Physica C 159 (1989) 141–149
North-Holland, Amsterdam

STRUCTURAL CHANGES OF THE SUPERCONDUCTOR $YBa_2Cu_3O_7$ BY COBALT SUBSTITUTION. A HIGH-RESOLUTION NEUTRON POWDER DIFFRACTION STUDY

R. SONNTAG, D. HOHLWEIN, A. HOSER and W. PRANDL
Institut für Kristallographie der Universität, 7400 Tübingen, Fed. Rep. Germany
(in collaboration with the Hahn–Meitner-Institut, Berlin)

W. SCHÄFER, R. KIEMEL, S. KEMMLER-SACK, S. LÖSCH and M. SCHLICHENMAIER
Institut für Anorganische Chemie der Universität Tübingen, Fed. Rep. Germany

A.W. HEWAT
Institut Laue–Langevin, Grenoble, France

Received 20 February 1989
Revised manuscript received 21 April 1989

The structure of cobalt substituted $YBa_2Cu_{3-x}Co_xO_{7\pm z}$ compounds with $x=0.05$, 0.1, 0.2, 0.3 and 0.65 was determined by high-resolution neutron powder diffraction at 5 and 300 K. The samples are superconducting up to $x=0.3$. $YBa_2Cu_{2.95}Co_{0.05}O_7$ has orthorhombic structure with space group Pmmm; all compounds with $x \geq 0.1$ have tetragonal structure with space group P4/mmm. The Rietveld refinements show clearly that the Co-atoms occupy only the Cu(1)-sites at (0, 0, 0), i.e. copper chain sites in the orthorhombic structure, for the whole composition range. The characteristic structural changes as a function of cobalt concentration and temperature are discussed. Along the *c*-axis the Cu(1) to O(2) distance is decreasing while the Cu(2) to O(2) distance is increasing as in the Co-free, oxygen deficient compounds. A charge transfer from the Cu/Co chains to the Cu planes is discussed. For the nonsuperconducting $YBa_2Cu_{2.35}Co_{0.65}O_{7.23}$ some magnetic peaks are observed.

1. Introduction

The structure of the 90 K high-T_c superconductor $YBa_2Cu_3O_7$ and related oxygen deficient compounds have been precisely determined by high resolution neutron powder diffraction [1–4]. One way to get more insight into structural stability and the conduction mechanism is by substitution of different kinds of atoms. The replacement of yttrium with rare-earth metal atoms (La, Nd, Sm, Eu, Gd, Ho, Er, Lu) has only a small influence on the superconducting transition temperature [5] while the substitution of copper atoms (Fe, Al, Ni, Zn, Co) has a great effect on T_c [6–18] which decreases to zero at substitutions as low as 5 to 15%. $YBa_2Cu_{3-x}A_xO_{7+\delta}$ with A=Ni, Zn remains orthorhombic in the composition range of $0 \leqslant x \leqslant 0.5$, while Fe, Al and Co substitution involves an orthorhombic-to-tetragonal phase transition at about $x=0.06$ (i.e. 2%) [6,10,13,16].

One important question concerning the substitution of copper atoms is whether the Cu(1) sites in the CuO chains or the Cu(2) sites in the CuO_2 planes will be involved. In the case of substitution by cobalt, neutron powder diffraction on $YBa_2Cu_{3-x}Co_xO_{7\pm z}$ has shown no evidence for an occupation of Co at the Cu(2) site for $x=0.2$ and 0.3, while for $x=0.8$ and 1.0 small values of 0.098(17) and 0.08(1) have been observed [6,16].

In this work we report high resolution neutron powder diffraction of $YBa_2Cu_{3-x}Co_xO_{7\pm z}$ for $x=0.05$, 0.1, 0.2, 0.3 and 0.65 at room temperature and at 5 K. In comparison to earlier work which was done partly only at room temperature and at much lower resolution, the structural parameters are determined for additional compositions and with higher precision. With that, the structural changes as a

function of composition can clearly be followed. Magnetic reflections are observed for $x=0.65$ but will only shortly be compared with other work [19,20].

2. Experimental

The samples were prepared from appropriate amounts of Y_2O_3, $BaCO_3$, CuO and Co powders by firing the intimate mixtures in corundum boats and in air for about 60 h at 900°C with several regrindings according to ref. [12]. Subsequently the samples were cooled down in oxygen atmosphere from 500°C to room temperature within 12 h. The oxygen content was determined from the mean oxidation state of Cu and Co as described in ref. [21]. The compositions determined were $YBa_2Cu_{3-x}Co_xO_z$ with $x=0.05$, 0.1, 0.2, 0.3, and 0.75; $z=6.88$, 6.89, 6.9, 6.93 and 6.99. We will see later that $x=0.65$ (value from the structure refinement) is the correct value and not 0.75 for the highest Co doped sample. The samples were checked on an X-ray powder diffractometer. All samples are single tetragonal phases with the exception of the lowest Co-doped sample which has a main single orthorhombic phase together with a tetragonal one of about 11%.

Electrical measurements [12] have shown superconductivity for $YBa_2Cu_{3-x}Co_xO_{7\pm z}$ for $x\leqslant 0.3$ and semiconducting behavior for the sample with $x=0.65$. Figure 1 shows the superconducting temperature T_c (midpoints) versus the Co content. For comparison we have included in the figure T_c values of Micele et al. [14] which were determined resistively as well as by AC and DC susceptibility measurements. There is a good agreement of the data.

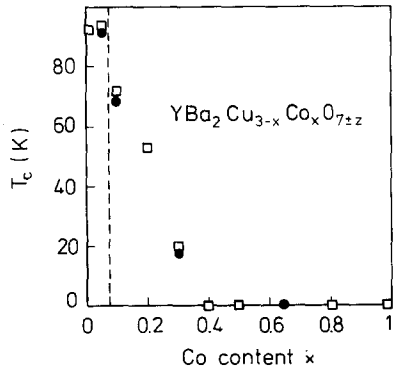

Fig. 1. T_c as a function of Co content x. For comparison with our data (●), values from Miceli et al. [14] are shown (□).

Neutron diffraction measurements were done at the high-resolution powder diffractometer D2B of the ILL in Grenoble [22]. The high intensity mode ($\alpha=35'$) was used to collect spectra at 5 and 300 K. The wavelength was 1.5946 Å. The 64 counters, spaced at 2.5° intervals, were moved by steps of 0.025° in a range of $2\theta\geqslant 2.5°$, giving a complete spectrum to 160° in 2θ. The samples were enclosed in a vanadium cylinder with diameter 16 mm and 40 mm height within a variable-temperature 'Orange' type helium cryostat.

3. Structure refinements and results

Rietveld profile refinements, including 145 reflections, were done for $YBa_2Cu_{3-x}Co_xO_{7\pm z}$ with $x=0.1$, 0.2, 0.3 and 0.65 for the 5 and 300 K data in the space group P4/mmm. The refined parameters are listed in table I for 300 K and table II for 5 K. There is a good agreement between the experimental data and the fitted profiles, illustrated by small R-values. A Rietveld fit with difference plot of $YBa_2Cu_{2.35}Co_{0.65}O_{7.23}$ at 300 K is shown in fig. 2.

In the refinements presented here, the cobalt atoms are constrained to the Cu(1) site, because refinements with cobalt on both sites yielded no significant values for the occupation factor on the Cu(2) site. Refinements of the occupation factor for cobalt agree well with the chemical preparation. Only in the Co-richest compound (a composition close to the phase boundary [12]) the refined value $x=0.65(1)$ deviates from the chemically one of 0.75. This is probably due to a small amount of CoO because an extraneous reflection is observed in the neutron diffraction pattern (fig. 2) at about $2\theta=43.5°$ which corresponds to the position of the 200-reflection of CoO.

The anisotropic temperature factor B_{11} for yttrium showed very small negative values at 5 K, but within the statistical error. So this temperature factor was fixed to zero.

For $YBa_2Cu_{2.95}Co_{0.05}O_7$ we started to refine the structure in the orthorhombic space group Pmmm, resulting in R-values two times larger than for the tetragonal compounds. The difference plot indicated

Table I
Refined parameters of tetragonal $YBa_2Cu_{3-x}Co_xO_{7\pm z}$ at 300 K. Space group P4/mmm. R_n, R_p, R_{exp} and R_{wp} are R-values of integrated intensities, profile, expected and weighted profile.

Co content x	0.1	0.2	0.3	0.65
Y (0.5/0.5/0.5)				
$B11$	0.26(3)	0.29(3)	0.36(3)	0.43(3)
$B33$	1.22(6)	1.60(7)	1.29(7)	1.19(8)
Ba (0.5/0.5/z)				
z	0.1853(1)	0.1862(2)	0.1869(2)	0.1873(2)
$B11$	1.40(4)	1.37(4)	0.98(4)	0.80(4)
$B33$	0.77(6)	0.95(7)	1.15(7)	1.03(7)
Cu(1) (0/0/0)				
occ.	0.89(1)	0.78(1)	0.69(1)	0.35(1)
$B11$	0.80(4)	0.74(5)	0.83(6)	1.18(9)
$B33$	0.70(6)	0.77(8)	0.63(8)	0.89(14)
Co(1) (0/0/0)				
occ.	0.11(1)	0.22(1)	0.31(1)	0.65(1)
$B11$	0.80(4)	0.74(5)	0.83(6)	1.18(9)
$B33$	0.70(6)	0.77(8)	0.63(8)	0.89(14)
Cu(2) (0/0/z)				
z	0.3567(1)	0.3577(1)	0.3584(1)	0.3602(1)
$B11$	0.62(2)	0.47(2)	0.53(2)	0.49(3)
$B33$	0.78(4)	0.98(5)	1.07(5)	1.07(5)
O(1) (0/0.5/0)				
occ.	1.07(1)	1.08(1)	1.13(1)	1.21(1)
$B11$	5.22(23)	5.46(24)	6.12(26)	6.23(26)
$B22$	2.27(15)	2.06(16)	1.81(16)	1.40(14)
$B33$	1.76(18)	2.33(21)	2.28(20)	1.41(18)
O(2) (0/0/z)				
z	0.1575(1)	0.1564(2)	0.1560(2)	0.1550(2)
occ.	1.86(1)	1.82(2)	1.91(2)	2.02(2)
$B11$	1.14(5)	1.36(6)	1.82(6)	2.42(8)
$B33$	1.11(8)	1.51(10)	1.48(10)	1.33(9)
O(3) (0/0.5/z)				
z	0.3780(1)	0.3782(1)	0.3781(1)	0.3778(1)
occ.	4.0	4.0	4.0	4.0
$B11$	0.58(3)	0.53(3)	0.51(4)	0.50(4)
$B22$	0.54(3)	0.57(3)	0.38(3)	0.47(4)
$B33$	1.12(4)	1.22(4)	1.14(4)	1.30(5)
a	3.86559(3)	3.86988(3)	3.87483(3)	3.88909(2)
c	11.6735(2)	11.6745(2)	11.6830(2)	11.6506(2)
R_n	3.8	4.3	4.4	3.7
R_p	9.2	9.9	9.6	10.1
R_{exp}	4.1	5.0	4.7	4.2
R_{wp}	10.5	11.1	10.8	10.7

small amounts of a tetragonal second phase (P4/mmm) and we refined both phases simultaneously. The amount of the tetragonal phase was found to be 11%. Because of this second (tetragonal) phase with its similar lattice parameters only isotropic thermal parameters could be refined. Table III shows the final parameters for the main orthorhombic phase $YBa_2Cu_{2.95}Co_{0.05}O_7$ at 5 and 300 K. The standard

Table II
Refined parameters of tetragonal $YBa_2Cu_{3-x}Co_xO_{7\pm z}$ at 5 K. Space group P4/mmm. R_n, R_p, R_{exp} and R_{wp} are R-values of integrated intensities, profile, expected and weighted profile.

Co content x	0.1	0.2	0.3	0.65
Y (0.5/0.5/0.5)				
$B11$	0.00	0.00	0.03(3)	0.00
$B33$	0.54(5)	1.01(6)	1.01(8)	0.85(6)
Ba (0.5/0.5/z)				
z	0.1837(1)	0.1850(1)	0.1859(2)	0.1878(2)
$B11$	1.11(3)	0.88(4)	0.65(4)	0.66(3)
$B33$	0.17(5)	0.60(6)	0.67(7)	0.87(6)
Cu(1) (0/0/0)				
occ.	0.90(1)	0.80(1)	0.70(1)	0.35(1)
$B11$	0.81(4)	0.87(5)	0.71(6)	0.86(7)
$B33$	0.36(6)	0.52(8)	0.35(9)	1.02(11)
Co(1) (0/0/0)				
occ.	0.10(1)	0.20(1)	0.30(1)	0.65(1)
$B11$	0.81(4)	0.87(5)	0.71(6)	0.86(7)
$B33$	0.36(6)	0.52(8)	0.35(9)	1.02(11)
Cu(2) (0/0/z)				
z	0.3560(1)	0.3570(1)	0.3581(1)	0.3599(1)
$B11$	0.42(2)	0.41(2)	0.29(2)	0.20(2)
$B33$	0.50(4)	0.61(4)	0.78(5)	0.85(4)
O(1) (0/0.5/0)				
occ.	1.05(1)	1.05(1)	1.11(1)	1.18(1)
$B11$	4.06(18)	3.92(22)	4.32(24)	4.94(20)
$B22$	1.66(13)	1.34(15)	1.50(16)	1.53(13)
$B33$	0.23(12)	1.74(20)	1.55(20)	0.99(15)
O(2) (0/0/z)				
z	0.1587(1)	0.1576(2)	0.1564(2)	0.1550(1)
occ.	1.97(1)	2.00(2)	1.98(2)	2.05(2)
$B11$	1.02(5)	1.30(6)	1.45(7)	2.35(7)
$B33$	0.68(7)	1.26(9)	1.36(11)	1.15(8)
O(3) (0/0.5/z)				
z	0.3778(1)	0.3780(1)	0.3778(1)	0.3771(1)
occ.	4.0	4.0	4.0	4.0
$B11$	0.27(3)	0.33(4)	0.26(4)	0.17(3)
$B22$	0.38(3)	0.28(3)	0.20(3)	0.18(3)
$B33$	1.01(3)	0.82(4)	0.79(4)	0.92(4)
a	3.85997(3)	3.86439(3)	3.86852(3)	3.88321(2)
c	11.6273(1)	11.6293(2)	11.6348(2)	11.6035(1)
R_n	3.7	4.2	3.7	3.9
R_p	8.0	9.3	9.6	9.3
R_{exp}	3.4	6.1	4.4	4.1
R_{wp}	9.4	10.5	11.3	10.5

deviations are considerably larger than for the pure tetragonal phases, because of parameter correlations with the minority phase.

In the compound $YBa_2Cu_{2.35}Co_{0.65}O_{7.23}$ we observed some weak magnetic reflections, as shown in fig. 3. The reflections $(\frac{1}{2}\ \frac{1}{2}\ \frac{1}{2})$ and $(\frac{1}{2}\ \frac{1}{2}\ \frac{3}{2})$ have also been found by Zolliker et al. [19] in $YBa_2Cu_{2.16}Co_{0.84}O_{7.32}$. They proposed a body-cen-

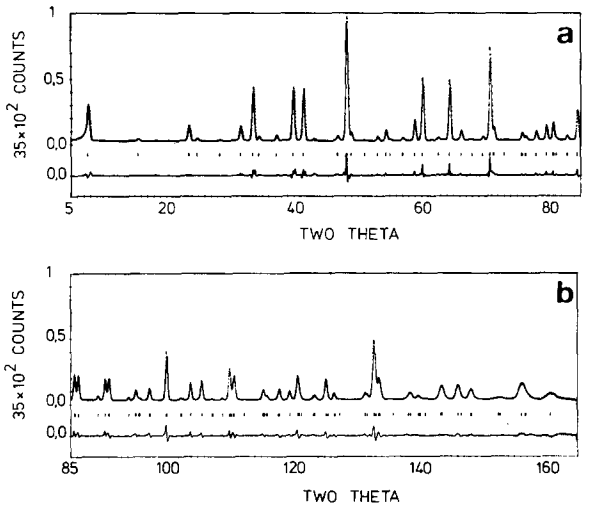

Fig. 2. Rietveld fit and difference plot of tetragonal $YBa_2Cu_{2.35}Co_{0.65}O_{7.23}$ at 300 K. Magnetic peaks in the range $17° \leqslant 2\theta \leqslant 21°$ are plotted enlarged in fig. 3. The extraneous peak at $2\theta = 43.5°$ is probably due to CoO (see text).

tered, tetragonal magnetic unit cell with $a_{mag} = a\sqrt{2}$ and $c_{mag} = 2c$. The magnetic moments are parallel to c and there is an antiferromagnetic ordering within both Cu and Co layers. The reflection $(\frac{1}{2}\ \frac{1}{2}\ 1)$, which has a different temperature behavior, has been observed also in an oxygen deficient compound with Co content $x = 0.2$ by Miceli et al. [20]. They proposed an antiferromagnetic structure with a zero moment at the Co atoms. For the discussion of corresponding magnetic structures, we refer to the literature mentioned.

4. Discussion

Starting from the well-known orthorhombic structure of the 90 K superconductor $YBa_2Cu_3O_7$, the Co substitution takes place exclusively in the CuO chains and not in the CuO_2 planes. The statistical errors of the structural parameters give an upper limit for Co in the CuO_2 planes of about 3% of all Co atoms.

For $x > 0.05$ the oxygen of the original chains $(0\ \frac{1}{2}\ 0)$ is distributed with equal probability also on $(\frac{1}{2}\ 0\ 0)$ giving a tetragonal lattice. With increasing x more oxygen is found at the O(1) sites, see tables I and II. This can be explained by the assumption that the Cu ions in Cu(1) are replaced by higher valent

Table III
Refined parameters of orthorhombic $YBa_2Cu_{2.95}Co_{0.05}O_7$ at 5 and 300 K. Space group Pmmm. R_n, R_p, R_{exp} and R_{wp} are R-values of integrated intensities, profile, expected and weighted profile. The results are from a 2 phase-refinement with a second tetragonal phase of 11% (see text). Parameter correlations with the minority phase explain the large standard deviations.

	300 K	5 K
Y (0.5/0.5/0.5)		
B	0.74(60)	0.43(58)
Ba (0.5/0.5/z)		
z	0.1854(36)	0.1852(56)
B	0.83(68)	0.47(66)
Cu(1) (0/0/0)		
occ.	0.95	0.95
B	0.58(60)	0.22(61)
Co(1) (0/0/0)		
occ.	0.05	0.05
B	0.58(60)	0.22(61)
Cu(2) (0/0/z)		
z	0.3562(21)	0.3556(22)
B	0.62(44)	0.25(46)
O(1) (0/0/z)		
z	0.1577(34)	0.1585(34)
occ.	1.91(40)	1.95(49)
B	0.82(1.09)	0.51(1.21)
O(2) (0.5/0/z)		
z	0.3781(34)	0.3775(35)
occ.	2.13(33)	2.16(39)
B	0.90(91)	0.62(99)
O(3) (0/0.5/z)		
z	0.3782(39)	0.3787(40)
occ.	1.91(38)	1.87(42)
B	0.36(1.01)	0.00(1.09)
O(4) (0/0.5/0)		
occ.	0.75(30)	0.70(32)
B	1.18(2.08)	0.22(2.07)
O(5) (0.5/0/0)		
occ.	0.30(40)	0.38(51)
B	9.2(21.0)	12.0(26.4)
a	3.8321(12)	3.8248(11)
b	3.8836(15)	3.8791(14)
c	11.6865(49)	11.6427(46)
R_n	5.1	4.5
R_p	9.9	10.4
R_{exp}	8.3	9.5
R_{wp}	11.8	12.64

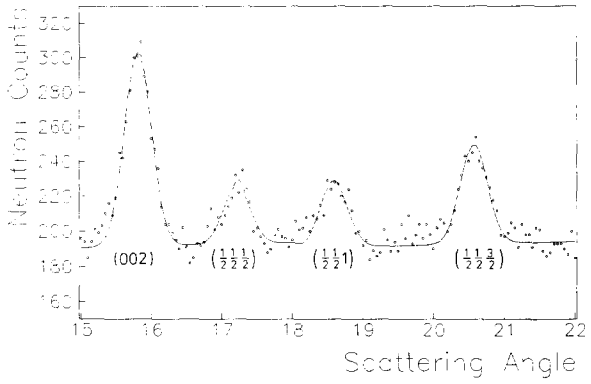

Fig. 3. Observed magnetic reflections (half integers) in $YBa_2Cu_{2.35}Co_{0.65}O_{7.23}$ at 5 K.

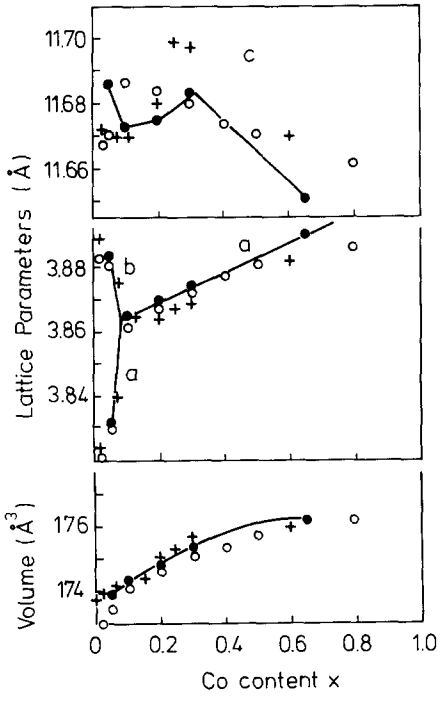

Fig. 4. Lattice parameters and cell volume of $YBa_2Cu_{3-x}Co_xO_{7\pm z}$ at 300 K as a function of cobalt content x (●). Values from Tarascon et al. (○) [6] and Shindo et al. (+) [17] are shown for comparison.

Co (probably Co^{3+}) which has the tendency for a higher coordination.

Figure 4 shows the lattice parameters and the unit cell volume as a function of the Co content. For comparison the results from Tarascon et al. [6] and Shindo et al. [17] at 300 K are included. Differences are probably due to a different oxygen content of the samples. The (nearly linear) increase in lattice parameter a with Co content and the monotonic increase of the unit cell volume can be explained by the uptake of oxygen atoms and larger cobalt to oxygen distances in the basal plane.

The lattice parameter c is growing slightly between $x=0.1$ to 0.3 and becomes shorter for larger x. To understand the structural changes in this direction we have to look at the individual atomic distances which are shown in fig. 5 and listed in table IV and V.

If we first regard the Cu/Co(1)–O(2) distance in fig. 5 we see a strong decrease with cobalt concentration, i.e., a stronger attraction between the O(2) atoms and the Co^{3+} ions. On the other hand the binding of the O(2) to Cu(2) is reduced and their distance is even more strongly increasing. The combination of these two effects gives a relative small increase of the Cu/Co(1)–Cu(2) distance.

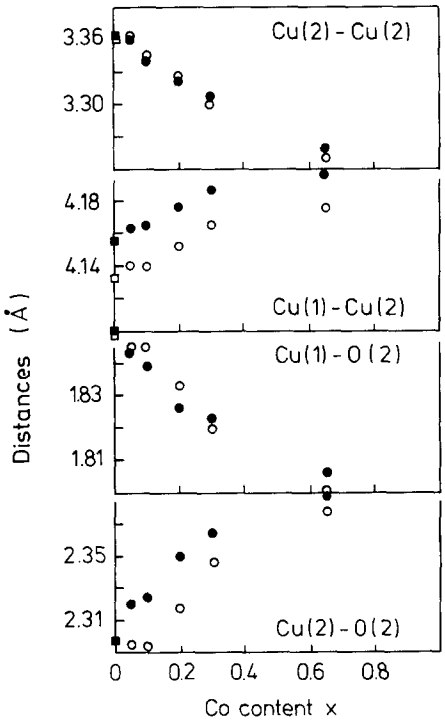

Fig. 5. Main atomic distances along the c axis in $YBa_2Cu_{3-x}Co_xO_{7\pm z}$ as a function of cobalt content x at 5 (○) and 300 (●) K. The orthorhombic values of $YBa_2Cu_3O_7$ (◨) are from M. Francois et al. [4].

Table IV
Atomic distances (Å) along the c axis in $YBa_2Cu_{3-x}Co_xO_{7\pm z}$ at 300 K.

Co content x	0.05	0.1	0.2	0.3	0.65
Cu/Co(1)-O(2)	1.84(4)	1.839(2)	1.826(2)	1.823(2)	1.806(2)
Cu(2)-O(2)	2.32(6)	2.325(4)	2.350(4)	2.365(4)	2.391(4)
Cu/Co(1)-Cu(2)	4.16(2)	4.164(1)	4.176(1)	4.187(1)	4.196(1)
Cu(2)-Cu(2)	3.36(5)	3.346(2)	3.323(2)	3.309(2)	3.258(2)
Ba-Ba	7.35(8)	7.347(5)	7.325(5)	7.314(2)	7.286(2)
Ba-Y	3.68(4)	3.674(2)	3.662(2)	3.657(2)	3.643(2)

Table V
Atomic distances (Å) along the c axis in $YBa_2Cu_{3-x}Co_xO_{7\pm z}$ at 5 K.

Co content x	0.05	0.1	0.2	0.3	0.65
Cu/Co(1)-O(2)	1.85(4)	1.845(1)	1.833(2)	1.820(2)	1.799(1)
Cu(2)-O(2)	2.30(6)	2.294(2)	2.319(3)	2.347(3)	2.378(2)
Cu/Co(1)-Cu(2)	4.14(3)	4.139(1)	4.152(1)	4.166(1)	4.176(1)
Cu(2)-Cu(2)	3.36(5)	3.349(2)	3.326(2)	3.302(2)	3.251(2)
Ba-Ba	7.33(10)	7.355(2)	7.326(2)	7.309(5)	7.275(5)
Ba-Y	3.67(7)	3.678(1)	3.663(1)	3.654(2)	3.637(2)

As a result of the diminishing attraction of the Cu(2) to the O(2) atoms (respectively layers) the two neighbouring Cu(2)-O(3) layers are contracted in direction to the intermediate Y^{3+} layer giving a shortening of the Cu(2)-Cu(2) distance (fig. 5). The increase of the lattice constant a with Co concentrations and the decrease of the nearest-neighbor Cu/Co to oxygen distance in c direction is also observed in the cobalt substituted $La_{1.8}Sr_{0.2}CuO_{4-z}$ compounds which we have studied recently [23].

It is interesting to note, that in pure $YBa_2Cu_3O_y$ comparable shifts of the distances in c-direction between Cu(1), Cu(2) and the oxygen atoms are observed with decreasing y [24]. Especially the distance Cu(1)-O(2) is decreasing and the Cu(2)-O(2) increasing as is the case with growing Co concentration (see fig. 6). This effect has been correlated with a rearrangement in the electronic structure; thus giving an explanation for the transition from a superconducting to a semiconducting material. Cava et al. [24] favour a charge transfer model to explain the superconducting properties of $YBa_2Cu_3O_y$. It is well established that the CuO_2 planes, which are a common structural component in all new high-T_c superconductors, play a central role

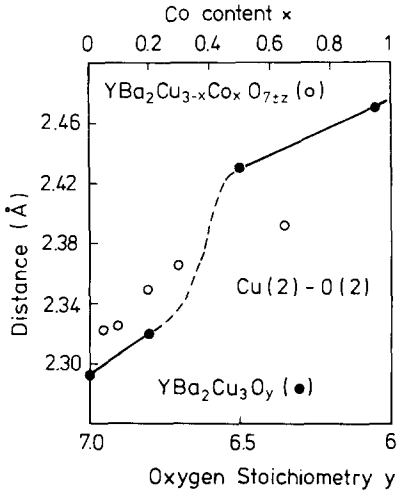

Fig. 6. Comparison of Cu(2)-O(2) distances in our Co doped sample (○) and in pure $YBa_2Cu_3O_y$ (●). The values for $YBa_2Cu_3O_y$ are from Cava et al. [24].

in superconductivity. The role of the CuO chains, as a secondary structural element, is that of a charge reservoir for the CuO_2 planes and controls its electron density. With decreasing oxygen concentration in $YBa_2Cu_3O_y$, an electron transfer from the chains to the planes takes place; consequently the hole con-

centration in the conducting planes decreases and the superconductivity vanishes.

In the system $YBa_2Cu_{3-x}Co_xO_{7\pm z}$ a transition from superconductivity to semiconduction is observed as well and it is tempting to assume that the observed positional shifts have a similar influence on the electrical properties of the CuO_2 planes. For example, fig. 6 shows the Cu(2)–O(2) distances both for Co doped and pure $YBa_2Cu_3O_y$. Instead of removing O^{2-}, Co^{3+} is substituted for copper of lower valence in the chains leading also to a (negative) charge transfer to the conducting plane. This diminishes the density of states (holes) at the Fermi surface and reduces T_c. In fig. 6 the scales of the abscissa are chosen in such a way that 1 Co atom corresponds to 1 oxygen, i.e., Co^{3+} replaces a Cu^{1+} ion.

By cooling down from 300 to 5 K, the relative decrease of the lattice parameter c is about 2.5 times larger then in lattice parameter a in contrast to the behavior with increasing Co content. This contraction along c can be described by a movement of two rigid structural units against each other (see fig. 7). One unit consists of the Cu/Co(1)–O(1)–O(2) layer and the second of all the other atoms. The main chemical bond between these units is the Cu(2)–O(2) bond which is strongly decreasing by cooling down. A similar behavior has been found in pure $YBa_2Cu_3O_y$ [4].

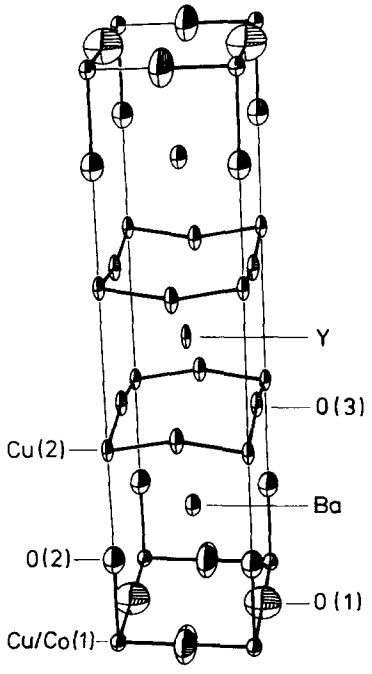

Fig. 7. Perspective view of the tetragonal structure of $YBa_2Cu_{2.7}Co_{0.3}O_{7.04}$ at 300 K.

In conclusion we emphasize that only a detailed knowledge of the structural parameters can be the basis of electronic models. Especially the complex behavior of the chemical bonds in c direction, as shown in fig. 5, cannot be deduced from the lattice constant c, has been done, e.g., in ref. [25].

Acknowledgement

This investigation has been supported financially by the Bundesminesterium für Forschung und Technologie under project number 03-PR1TUE-6.

References

[1] J.J. Capponi, C. Chaillout, A.W. Hewat, P. Lejay, M. Marezio, N. Nguyen, B. Raveau, J.L. Soubeyroux, J.L. Tholence and R. Tournier, Europhys. Lett. 3 (1987) 1301.
[2] F. Beech, S. Miraglia, A. Santoro and R.S. Roth, Phys. Rev. B 35 (1987) 8778.
[3] J.Y. Henry, P. Burlet, A. Bourret, G. Roult, P. Bacher, M.J.G.M. Jurgens and J. Rossat-Mignod, Sol. State Phys. 7 (1987) 1037.
[4] M. Francois, A. Junod, K. Yvon, A.W. Hewat, J.J. Capponi, P. Strobel, M. Marezio and P. Fischer, Sol. State Phys. 10 (1988) 1117.
[5] P.H. Hor, R.L. Meng, Y.Q. Wang, L. Gao, Z.J. Huang, J. Bechtold, K. Forster and C.W. Chu, Phys. Rev. Lett. 58 (1987) 1891.
[6] J.M. Tarascon, P. Barboux, P.F. Miceli, L.H. Greene, G.W. Hull, M. Eibschutz and S.A. Sunshine, Phys. Rev. B 37 (1988) 7458.
[7] J.M. Tarascon, L.H. Greene, P. Barboux, W.R. McKinnon, G.W. Hull, T.P. Orlando, K.A. Delin, S. Foner and E.J. McNiff Jr., Phys. Rev. B 36 (1987) 8393.
[8] T. Siegrist, L.F. Schneemeyer, J.V. Wasczcak, N.P. Singh, R.L. Opila, B. Batlogg, L.W. Rupp and D.W. Murphy, Phys. Rev. B 36 (1987) 8365.
[9] Y. Oda, H. Fujita, H. Toyoda, T. Kaneko, T. Kohara, I. Nakada and K. Asayama, Jpn. J. Appl. Phys. 26 (1987) L1660.
[10] G. Xiao, M.Z. Cieplak, A. Gavrin, F.H. Streitz, A. Bakshai and C.L. Chien, Phys. Rev. Lett. 60 (1988) 1446.
[11] G. Xiao, M.Z. Cieplak, D. Musser, A. Gavrin, F.H. Streitz, C.L. Chien, J.J. Rhyne and J.A. Gotaas, Nature 332 (1988) 238.

[12] R. Kiemel, W. Schäfer, S. Kemmler-Sack, G. Kruschel and B. Elschner, J. Less-Common Metals 143 (1988) L11.
[13] I. Sankawa, M. Sato and T. Konaka, Jpn. J. Appl. Phys. 27 (1988) L28.
[14] P.F. Miceli, J.M. Tarascon, L.H. Greene, P. Barboux, F.J. Rotella and J.D. Jorgensen, Phys. Rev. B 37 (1988) 5932.
[15] T. Kajitani, K. Kusaba, M. Kikuchi, Y. Syono and M. Hirabayashi, Jpn. J. Appl. Phys. 26 (1987) L1727.
[16] T. Kajitani, K. Kusaba, M. Kikuchi, Y. Syono and M. Hirabayashi, Jpn. J. Appl. Phys. 27 (1988) L354.
[17] D. Shindo, K. Hiraga, M. Hirabayashi, A. Tokiwa, M. Kikuchi, Y. Syono, O. Nakatsu, N. Kobayashi, Y. Muto and E. Aoyagi, Jpn. J. Appl. Phys. 26 (1987) L1667.
[18] J.F. Bringley, T.-M. Chen, B.A. Averill, K.M. Wong and S.J. Poon, Phys. Rev. B 38 (1988) 2432.
[19] P. Zolliker, D.E. Crox, J.M. Tranquada and G. Shirane, Phys. Rev. B 38 (1988) 6575.
[20] P.F. Miceli, J.M. Tarascon, L.H. Greene, P. Barboux, M. Giroud, D.A. Neumann, J.J. Rhyne, L.F. Schneemeyer and J.V. Waszczak, Phys. Rev. B 38 (1988) 9209.
[21] W. Schäfer, J. Maier-Rosenkranz, S. Lösch, R. Kiemel, W. Wischert and S. Kemmler-Sack, J. Less-Common Metals 142 (1988) L5.
[22] A.W. Hewat, Mat. Science Forum 9 (1986) 69.
[23] D. Hohlwein, A. Hoser, R. Sonntag, W. Prandl, W. Schäfer, R. Kiemel, S. Kemmler-Sack and A.W. Hewat, Physica B 156 & 157 (1989) 893.
[24] R.J. Cava, B. Battlog, K.M. Rabe, E.A. Rietman, P. Gallagher and L.W. Rupp, Physica C 156 (1988) 523.
[25] R. Aoki, S. Takahashi, H. Murakami, T. Nakamura, T. Nakamura, Y. Takagi and R. Liang, Physica C 156 (1988) 405.